UTADEO
UNIVERSIDAD DE BOGOTÁ JORGE TADEO LOZANO
FACULTAD DE CIENCIAS NATURALES E INGENIERÍA

SEMILLERO DE NANOBIOINGENIERÍA
Semillero de Investigación y Creación del Departamento de Ingeniería Enfocado en el Trabajo con Nanotecnología

OPTIMIZATION OF NANOSTRUCTURED MATERIAL PRODUCTION COMPOSED BY NYLON NANOWIRES WITH GRAPHENE: A RESPONSE SURFACE METHODOLOGY APPROACH

JORGE SEBASTIÁN COBA DAZA
KATHERINE HELENA HERNÁNDEZ BAUTISTA

Partial Fulfillment of the
Requirements for the degree in Chemical Engineering

Director: Alis Yovana Pataquiva-Mateus, Chem. Eng., MSc., PhD.

UNIVERSIDAD DE BOGOTÁ JORGE TADEO LOZANO
FACULTAD DE CIENCIAS NATURALES E INGENIERÍA
INGENIERÍA QUÍMICA
28th SEPTEMBER, 2017
BOGOTA DC.

CONTENT TABLE

List of figures

List of tables

OPTIMIZATION OF NANOSTRUCTURED MATERIAL PRODUCTION COMPOSED BY NYLON NANOWIRES WITH GRAPHENE: A RESPONSE SURFACE METHODOLOGY APPROACH

OPTIMIZACIÓN POR LA METODOLOGÍA DE SUPERFICIE DE RESPUESTA DE LA FABRICACIÓN DE UN MATERIAL NANOESTRUCTURADO COMPUESTO DE NANOHILOS DE NYLON CON GRAFENO

ABSTRACT

In the present study, nylon nanowires/graphene composite was produced via electrospinning technique and electrochemical exfoliation process making use of an optimization process. Pristine and composite materials were studied by morphological and structural (SEM, AFM), chemical (FTIR, XRD), UV blocking (UV-visible spectroscopy) and antimicrobial activity. Experimental design gave the optimal parameters to synthesize graphene and nylon nanowires such as: for the electrochemical exfoliation a polarization potential of 11.45 V and and a 0.68 M of (NH4)2SO4 concentration in the graphene production, while for the electrospinnign process an electric field of 27 kV/11.40 cm and a pumping rate of 2.30 mL/h to produce nylon-based nanofibers ere set. Characterization analysis revealed that electrochemical exfoliation process produced high quality graphene (single and few layers) with 33 to 71 nm of layer thickness. Optimal nylon nanowires showed 65.83±12 nm of diameter, and composite material was produced mixing both materials under optimal conditions and extruded employing the electrospinning technique. This material showed interesting properties UV blocking properties in order to be used in smart textiles.

Keywords: Graphene, electrochemical exfoliation, electrospinning, nanowires, surface response, composite material.

RESUMEN

En el presente estudio el compuesto de nanohilos de nylon/grafeno fue producido por medio del proceso de electrohilado y el de exfoliación electroquímica. Los materiales fabricados fueron estudiados para conocer sus propiedades morfológicas y estructurales (SEM, AFM), sus características químicas (FTIR, XRD), su capacidad de bloqueo de rayos UV (Espectroscopia UV-visible) y actividad. El diseño experimental otorgó los parámetros óptimos para la producción de grafeno y nanohilos de nylon: 11.45 V y concentración de $(NH_4)_2SO_4$ igual a 0.68 M para la producción de grafeno; y voltaje aplicado de 27 kV, flujo de 2.3 mL/h y distancia ajuga al colector igual a 11.40 cm para la producción de nanohilos de nylon. Los resultados de caracterización revelaron que el proceso de exfoliación electroquímica produce grafeno de alta calidad (una a pocas capas) con diámetros desde 33 hasta 77 nm. El material de nanohilos óptimo presenta un diámetro promedio de 65.83 ± 12 nm y el material compuesto fue producido mezclando las dos condiciones óptimas de ambos materiales en el electrohilador. El material compuesto de nanohilos de nylon con grafeno presenta interesantes propiedades como bloqueo de rayos UV y la capacidad antimicrobiana como una propuesta atractiva en el campo de los textiles inteligentes.

Palabras clave: Grafeno, exfoliación electroquímica, electrospinning, nanohilos, superficie de respuesta, material compuesto.

1. INTRODUCTION

Graphene is a material that consists of a two-dimensional (2D) sheet of covalently bonded carbon atoms and sp^2 atoms in a hexagonal lattice (Lee, Wei, Kysar, & Hone, 2008). Since graphene was discovered in 2004 (Novoselov et al., 2004; Ray, 2015b) its properties and possible applications have been studied. These properties are attractive because of their performance in different fields. Graphene has Young's modulus of 1.0 TPa (Ray, 2015a), ~ 2630 $m^2 g^{-1}$ of specific surface area (Stoller, Park, Zhu, An, & Ruoff, 2008), conductivity of 0.1 $S\, m^{-1}$, and its thermal conductivity is fivefold higher than cooper and it is about 3000 $W\, m^{-1} K^{-1}$ (Ray, 2015a; Stankovich et al., 2006).

There are different types of synthesis to produce graphene such as mechanical exfoliation (Lu, Yu, Huang, & Ruoff, 1999), electrochemical expansion (Zhong & Swager, 2012), chemical deposition (X. Li et al., 2011), Hummer's method (Jr & Offeman, 1958), epitaxial growth (Chen, Xue, & Komarneni, 2017) and electrochemical exfoliation (Jibrael & Mohammed, 2016a). The selection of the best synthesis is based on the quality of graphene that depends on variables such as speed, simplicity and yield percentage which it is desired to obtain, among others (Chen et al., 2017). Electrochemical exfoliation is advisable for the mass production of graphene and has many advantages above other processing routes (Zhong, Tian, Simon, & Li, 2015). Also, this synthesis allows to produce functionalized graphene which can be used in several industrial applications such as electronics, coatings, nanocomposite and energy storage (Yu, Lowe, Simon, & Zhong, 2015). On the other hand, electrochemical exfoliation based on a solution of $(NH_4)_2SO_4$, an environmental friendly reagent, is low cost and easily-made synthesis for the production of high quality graphene (Chen et al., 2017; Parvez et al., 2014). A suitable combination of voltage and salt concentration makes the process efficient in terms of percent yield and morphology; in this order of ideas, it is important to use an optimization model like central composite design (CCD) to find optimal values for those variables; even more, the amount of researches that involve an optimization process is limited (Scopus, n.d.).

When graphene is added to a polymeric matrix, a lot of properties might be increased and the possible applications are even more than pristine graphene (Ji, Xu, Zhang, Cui, & Liu, 2016). Some of these are high thermal stability, high Young's modulus, high tensile strength, high conductivity, high fatigue life, high sensitivity, and important antibacterial and hydrophobicity properties (Ji et al., 2016; Ren et al., 2013). To improve those properties, there are different ways to fabricate polymer/graphene composite material as solvent processing, melt mixing, *in situ* polymerization, spraying and so on (Ji et al., 2016). The solvent processing method includes electrospinning technique, with it is possible to produce nanometric materials using the electrical forces between the polymer surface's and the collector, causing an electrically charged cone (known as Taylor's cone) to be ejected in form of a wire (Deitzel, 2002; El-Newehy, Al-Deyab, Kenawy, & Abdel-Megeed, 2011; Nirmala, Navamathavan, El-Newehy, & Kim, 2011; Pedicini & Farris, 2004; Reneker & Chun, 1996; S. Zhang, Shim, & Kim, 2009).

Nanocomposite materials fabrication via electrospinning process is fast and applied to wide range of applications, some authors have shown studies in smart textiles, energy storage, sensors, filters, tissue engineering and in cosmetic industry (Huang, Zhang, Kotaki, & Ramakrishna, 2003; Laurencin, Ambrosio, Borden, & Cooper Jr, 1999). In this work, nylon nanowires/graphene composite was investigated and optimized showing interesting properties as antibacterial and UV blocking characteristics, obtaining a potential material in smart textiles applications.

2. METHODOLOGY

2.1. Graphene synthesis

Graphene was synthetized from electrochemical exfoliation method with graphite mines in electrolytic solution of ammonia sulfate. This methodology was based and modified from Jibrael and coworkers (Jibrael & Mohammed, 2016b) and is based on the immersion of the electrodes (graphite mines number 2B of 2 mm of diameter, Faber Castell®) in an electrolysis cell. Conditions of concentration of $(NH_4)_2SO_4$ and voltage were provided by experimental design (ED) whose response is percent yield. Table 1 shows current and codded factors used in the experimental design (which will be explained in deep in section 2.4). Once the exfoliation process was finished, reaction products were centrifuged at 4000 rpm during 45 min, then the precipitated was dried in oven at 200 °C during 1 h and obtained powder that was macerated with agate mortar. Finally, exfoliation products were characterized morphologically employing a scanning electron microscope (SEM) and the diameter of flakes observed was measured by ImageJ software (Schneider, Rasband, & Eliceiri, 2012)

Table 1 Values of the central composite experimental design for the graphene production via electrochemical process

Factor	Coded factor		
	-1	0	1
Voltage (V)	8	10	12
Concentration of $(NH_4)_2SO_4$	0.1	0.55	1

2.2. Fabrication of nylon nanowires

2.2.1. Preparation of polymeric solution

Commercial nylon number 6 was dissolved into formic acid (85 % v/v) at concentration of 10 % w/v. The storage of the solution and experiments were performed at room temperature.

2.2.2. Electrospinning process

Polymeric solution of nylon was placed into a syringe of 20 mL with a needle of 2 mm of diameter. Positive electrode of the power supply was connected to needle while negative electrode was attached to a collector (aluminum foil) as it is shown in Figure 1. Conditions of voltage, flow and collector-needle distance were used in order to carry out an optimization process by surface

response methodology, which had average diameter as a response. Table 2 shows codded and current values used in ED. The process was carried out on the NANOFIB 100 equipment of QUBITeXp®.

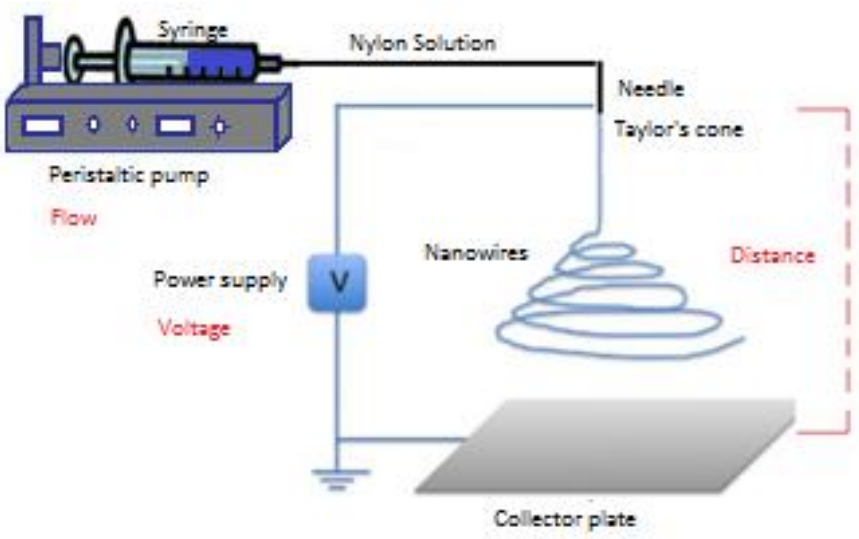

Fig. 1 Basic scheme of electrospinning performance used in nylon nanowires production. Flow, voltage and distance (collector-needle) were the variables used in the experimental design with wires diameter as response.

Table 2 Values of the central composite experimental design for the nanowires production.

Factor	Coded Factor		
	-1	0	1
Voltage (kV)	27	28	29
Flow (mL/h)	1	2	3
Collector needle distance (cm)	9	11	13

2.3. Fabrication of nylon nanowires/graphene composite

Graphene produced using optimal conditions was added to a solution of nylon in formic acid in proportion of 1% w/v. The mixture was homogenized and taken in a 20 mL syringe, immediately syringe was attached to electrospinning equipment and optimal conditions given by the response surface were adjusted to produce nylon nanowires/graphene composite.

2.4. Response surface methodology

Response surface methodology was used to analyze both experimental designs which are the fabrication of graphene and nylon nanowires production; for such purpose, central composite design of experiments (CCD) was used by the aid of Design Expert software (version 6.0.8, Stat-Ease Inc., Minneapolis, MN, USA). Second order model was adjusted for the experimental data for both process, and the reliability of the models were verified by determination coefficient (R^2) and ANOVA analysis. Finally, graphene production model was maximized to find optimal value

that gives a higher percent of yield in the range of evaluated conditions, also for nylon nanowires model a minimization was used to find the less possible mean diameter.

2.5. Characterization

2.5.1. Scanning electron microscopy (SEM)

Morphological characteristics of graphene, nylon nanowires and nylon nanowires/graphene composite were studied using a scanning electron microscope (JEOL JSM-6490LV). Graphene sheets thickness and nanowires diameter were measured from micrographs using ImageJ software 1.47V (NIH, USA) (Schneider et al., 2012). Samples were directed metalized with gold (100 Å, uniform covering) in Desk IV metallizer.

2.5.2. Atomic Force Microscopy (AFM)

An AFM device (Asylum Research, MFP-3D) in tapping mode was used to imaging and analyzing the nylon nanowires/graphene composite. Sample of 1x1 cm^2 was glued with a tape to a metallic disc, silicon tape was used to morphological study. Roughness parameters were measured with Gwyddion software (Necas & Klapetek, 2012).

2.5.3. Fourier transform infrared spectroscopy (FTIR)

Chemical features were studied using Fourier transform infrared analysis obtained using Ainfra Red Spectrophotometer (Agilent Cary 630 FTIR) with attenuate total reflectance (ATR) to confirm functional groups presents in the sample. Solution of graphene in water (0.1 g/mL) and polymeric films were used in the test to confirm present functional groups.

2.5.4. X-Ray diffraction (XRD)

X-Ray diffraction patterns of graphite, graphene, nylon nanowires, and nylon nanowires/graphene composite were obtained using PANalytical X'Pert PRO MPD with Cu anode (λ=1.54056 Å), step size of 0.02° and step time of 2° min^{-1}. Diffraction patterns were taken at room temperature.

2.5.5. Antimicrobial activity

To perform the antibiogram, 10 g of TSA agar was dissolved in 250 mL of distillate water, the solution was brought to a boil. Solution, petri plates, cotton swabs were sterilized. Liquid culture of *Micrococcus luteus* was used in the study. 100 µL of culture was inoculated in a petri dish with TSA, well diffusion method was used. Three samples of 1 cm^2 were put in the petri plate with the culture and finally, all were inoculated at 30°C for 24 h.

2.5.6. UV Blocking test

UV–visible spectrometer (Thermo Scientific, Evolution 300) was used to investigate the ability of nylon nanowires/graphene composite to blocking UV rays. Samples with 2 x 2 cm were directly used in the 200 to 800 nm of wavelength range following the method proposed by Pant and coworkers in their work (Pant et al., 2011).

3. RESULTS AND DISCUSSION

3.1. Optimization of graphene production

Surface response methodology and central composed design were used to investigate the effect of variables voltage and concentration of electrolytic solution ($(NH_4)_2SO_4$) in exfoliation of graphite to graphene production. Table 3 shows results obtained for each experiment.

Table 3 Results of Central composed design for graphene production by electrochemical exfoliation and the observed yield for each experiment

Experiment No.	Voltage (V) x_1	Concentration (NH4)2SO4 [M] x_2	Yield (%)
1	8	0.1	1.07
2	12	0.1	55.44
3	8	1	7.03
4	12	1	58.42
5	8	0.55	34.72
6	12	0.55	63.73
7	10	0.1	60.11
8	10	1	63.78
9	10	0.55	62.18
10	10	0.55	65.80
11	10	0.55	60.10
12	10	0.55	56.19
13	10	0.55	48.55

Equation 1 represents a second order polynomial model that correlates voltage x_1 (V) and concentration x_2 [M] with yield Y(%).

$$Y(\%) = -566.89 + 111.31\,x_1 + 52.74\,x_2 - 4.98\,x_1^2 - 36.23\,x_2^2 - 0.82\,x_1\,x_2 \quad (1)$$

Analysis of variance (ANOVA) confirms the significance of the model. In Table 4 ANOVA is shown, p-value $= 0.0047$ indicates that the model is statistically significant because it is $p<0.05$.

The lack of fit value (0.1051) and R^2 0.9809 make evident that model is well adjusted to experimental data and it can be used if the purpose is to know the yield under given conditions.

Table 4 ANOVA analysis for graphene production by the yield model.

Source	Sum of squares	DF	Mean square	F Value	P-Value
Model	4882.21	5	976.44	9.75	0.0047
x_1	3027.63	1	3027.63	30.24	0.0009
x_2	26.49	1	26.49	0.26	0.6228
x_1^2	1106.47	1	1106.47	11.05	0.0127
x_2^2	147.07	1	147.07	1.47	0.2648
$x_1 x_2$	2.22	1	2.22	0.022	0.8859
Residual	700.88	7	100.13		
Lack of Fit	527.22	3	175.74	4.05	0.1051
Pure Error	173.66	4	43.42		
Cor Total	5583.09	12			

With this experimental model, the goal was to maximize percent of yield (Y) to bring the optimal values, Figure 2 shows the surface response.

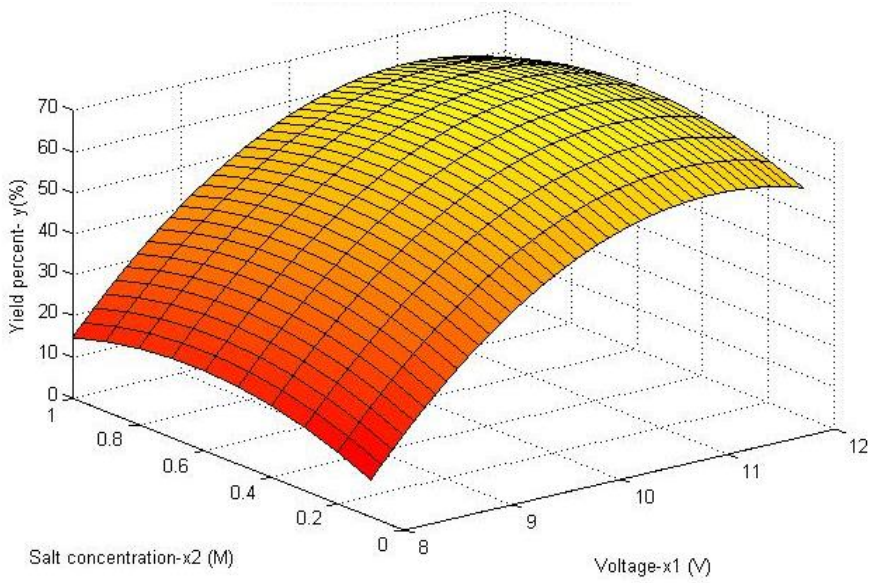

Fig. 2 Surface response for graphene production by chemical exfoliation synthesis.

Parvez and coworkers (Parvez et al., 2014) investigated the effect of concentration of $(NH_4)_2SO_4$ in electrochemical exfoliation for graphene production. Results demonstrated that the concentration of salt and voltage produce low yield (~ 5%), which suggests that a limited number

of ions are available to exfoliate. In contrast when concentration increases to 1.0 M, the yield is ~ 75%, also when concentration is high (3 to 5 M) the yield was <50%, and it is because the formation of OH^- ions was suppressed because of the low water content and $SO4^{2-}$ ion intercalation processes are expected to be relatively slow. Those results are well consistent with the results in the present work, for this reason, table 5 shows the optimal values that makes the yield be a maximum for the process.

Table 5 Optimal values from maximized graphene production model

Voltage (V)	11.45
Concentration (M)	0.68
Yield (%)	67.21 ± 10.01

3.1.1. Effect of process parameters

3.1.1.1. Effect of voltage

Effect of variable voltage is shown in Figure 3, as the voltage increases at concentration constant (0.68 M), yield also increases until the value of 11.45 V, and it is because that with higher voltage used the mine break and finished exfoliation process. Using maximum voltage (12 V) resulted in a decrease of 3.33% respect to maximum value in terms of yield.

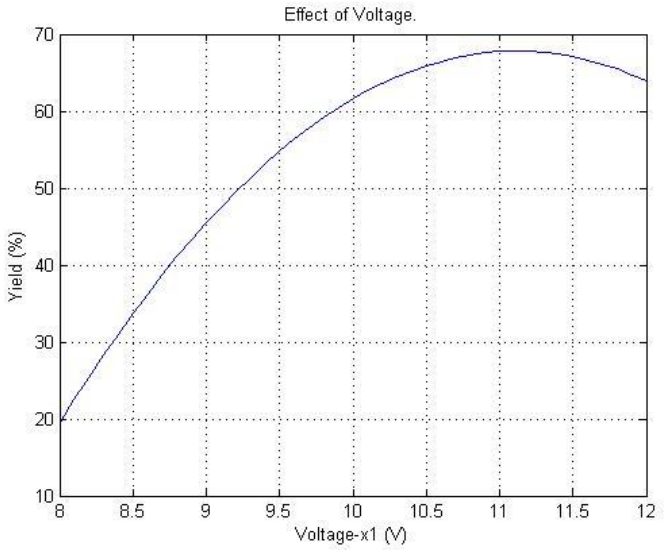

Fig. 3 Effect of voltage in electrochemical exfoliation process at constant concentration of (NH4)2SO4 equal to 0.68 M

3.1.1.2. Effect of salt concentration

The $(NH_4)_2SO_4$ concentration had a similar effect than voltage. Figure 4 shows that higher salt concentration than 0.60 M induces electrode (graphite mine) to break, finishing faster the

exfoliation process. Using maximum concentration (1 M) yield decreases in 5.60% respect to maximum value.

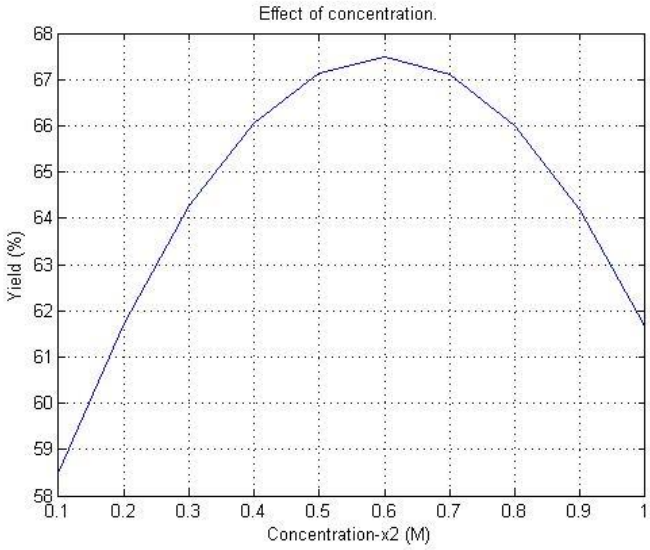

Fig. 4 Effect of concentration of (NH4)2SO4 in electrochemical exfoliation process at constant voltage equal to 11.45 V

3.2. Optimization of nylon nanowires production

The effect of variables: voltage, flow and collector-needle distance for nylon nanowires was studied using the central composite design (CCD). Table 6 shows the results obtained for each experiment.

Table 6 Results of Central composed design for nylon nanowires production by electrospinning technique and the observed mean diameter for each experiment.

Experiment No.	Voltage (kV) z_1	Flow (mL/h) z_2	collector-needle distance (cm) z_3	Mean diameter(nm) D
1	27	1	9	93
2	29	1	9	87
3	27	3	9	85
4	29	3	9	80
5	27	1	13	66
6	29	1	13	91
7	27	3	13	73
8	29	3	13	92
9	27	2	11	76
10	29	2	11	80
11	28	1	11	110
12	28	3	11	105
13	28	2	9	124
14	28	2	13	138
15	28	2	11	113
16	28	2	11	100
17	28	2	11	80
18	28	2	11	103
19	28	2	11	95

Equation 2 represents a second order polynomial model that correlates mean diameter D (nm) with Voltage z_1 (kV), Flow z_2 (mL/h) and collector-needle distance z_3 (cm)

$$D = -24896.68 + 1861.61\, z_1 + 17.80\, z_2 - 205.01\, z_3 - 33.82\, z_1^2 - 4.32\, z_2^2 + 4.79\, z_3^2 - 0.62\, z_1 z_2 + 3.43\, z_1\, z_3 + 1.43\, z_2\, z_3 \quad (2)$$

To confirm the reliability of model, ANOVA analysis was used. Table 7 shows the ANOVA for quadratic model of nylon nanowires production, P-value equal to 0.0047 probes that the model is statistically significant (*p*-value must be less than *0.05*). The lack of fit value equal to 0.52 and coefficient of determination (R^2) equal to 0.96.

Table 7ANOVA analysis for nylon nanowires production as mean diameter as response.

Source	Sum of Squares	DF	Mean Squares	F Value	P-value
Modelo	4655.11	9	517.23	3.54	0.04
z_1	136.90	1	136.90	0.94	0.36
z_2	14.40	1	14.40	0.10	0.76
z_3	8.10	1	8.10	0.06	0.82
z_1^2	3127.12	1	3127.12	21.38	0.00
z_2^2	51.23	1	51.23	0.35	0.57
z_3^2	1004.14	1	1004.14	6.86	0.03
$z_1 z_2$	3.13	1	3.13	0.02	0.89
$z_1 z_3$	378.13	1	378.13	2.58	0.14
$z_2 z_3$	66.13	1	66.13	0.45	0.52
Residual	1316.58	9	146.29		
Lack of Fit	729.78	5	145.96	0.99	0.52
Pure Error	586.80	4	146.70		
Cor Total	5971.68	18			

This model was minimized to find values of variables that makes average diameter minimum. Figure 5 shows the surface response of the model and Table 8 shows optimal values.

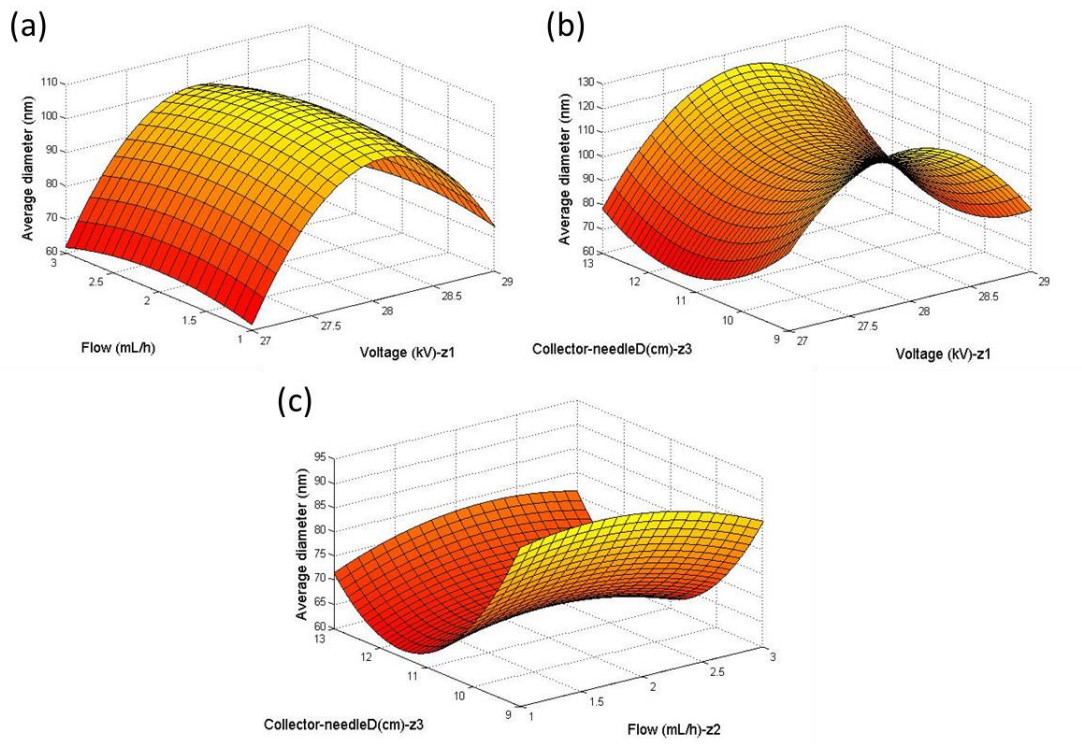

Fig. 5 Surface response representation for nylon nanowires production showing effects between interactions of (a) Flow and voltage with constant distance equal to 11.40 cm, (b) Collector-needle distance and voltage with constant flow equal to 2.30 mL/h and (c) collector needle distance and flow with constant voltage equal to 27 kV.

Table 8 Optimal values from minimized nylon nanowires production model

Voltage (kV)	27.00
Flow (mL/h)	2.30
Collector-needle distance (cm)	11.40
Average diameter (nm)	65.83 ± 12.09

3.2.1. Effect of process parameters

3.2.1.1. Effect of voltage

Figure 6 shows effect of voltage in average diameter of nanowires, there is a parabolic behavior with inflection point in 28.1 kV on the X axis, while the extremes of the range evaluated predict a smaller fiber diameter. This finding supports Zhang´s and coworkers study (C. Zhang, Yuan, Wu, Han, & Sheng, 2005) where lower voltage was applied decreasing wire diameter, and a narrow distribution of fiber diameters were observed. In addition, data reported by Yuan et al. (Ki et al.,

2005) showed that high voltage favors the narrowing of wire diameter. As is presented in Table 8, optimal value is which one that makes the fiber had minimum diameter using the smallest possible applied voltage, bringing to the process the best alternative in terms of input energy.

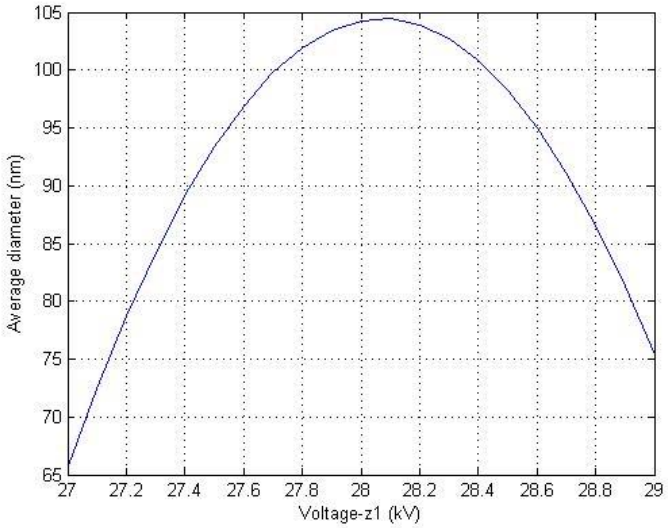

Fig. 6 Effect of Voltage with flow and collector-needle distance constant equal to 2.3 mL/h and 11 cm respectively in average diameter.

3.2.1.2. Effect of flow

Effect of flow in electrospinning process is shown in Figure 7, as can be seen, as the flow increases, average diameter presents a quasi-constant pattern, it means that in comparison with the other effects, flow is not considered a crucial parameter. Yuan and coworkers (Yuan, Zhang, Dong, & Sheng, 2004) reports that bead-wires formation (drop-like) is caused because of the higher flow rate, and recommend using a slow flow rate in order to the solvent have enough time for evaporate.

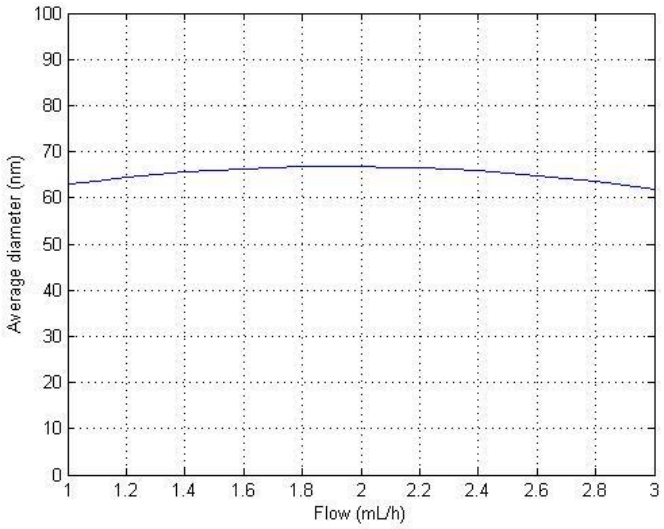

Fig. 7 Effect of flow with voltage and collector-needle distance constant equal to 27 kV and 11 cm respectively in average diameter.

3.2.1.3. Effect of collector-needle distance

Figure 8 shows effect of collector-needle distance in fiber diameter. In this case, when the collector needle distance increase, diameter of nanowires decreases and it is well consistent with literature (Z. Li & Wang, 2013) where it is demonstrated that if the distance is too long, bead-wires can be obtained and diameter are increased, while if the distance is too short there is no enough time for the solidification of the fiber before reaching the collector (Ki et al., 2005; Yuan et al., 2004).

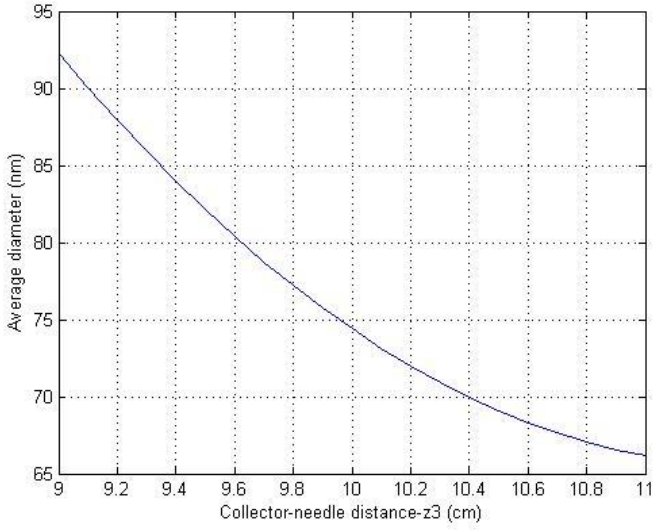

Fig. 8 Effect of Collector-needle distance with voltage and flow constant equal to 27 kV and 2.3 mL/h respectively in average diameter.

3.3. Characterization of materials obtained

3.3.1. Graphene characterization

3.3.1.1. Scanning electron microscopy (SEM)

Figure 9 shows micrographs of single layer (A, red line) and few layers (B) of graphene obtained by electrochemical exfoliation. It was measured that thickness of graphene sheets are in a range of 33-70 nm, those results confirm previous images reported in literature (Parvez et al., 2014; Wang, Manga, Bao, & Loh, 2011; Zhong & Swager, 2012).

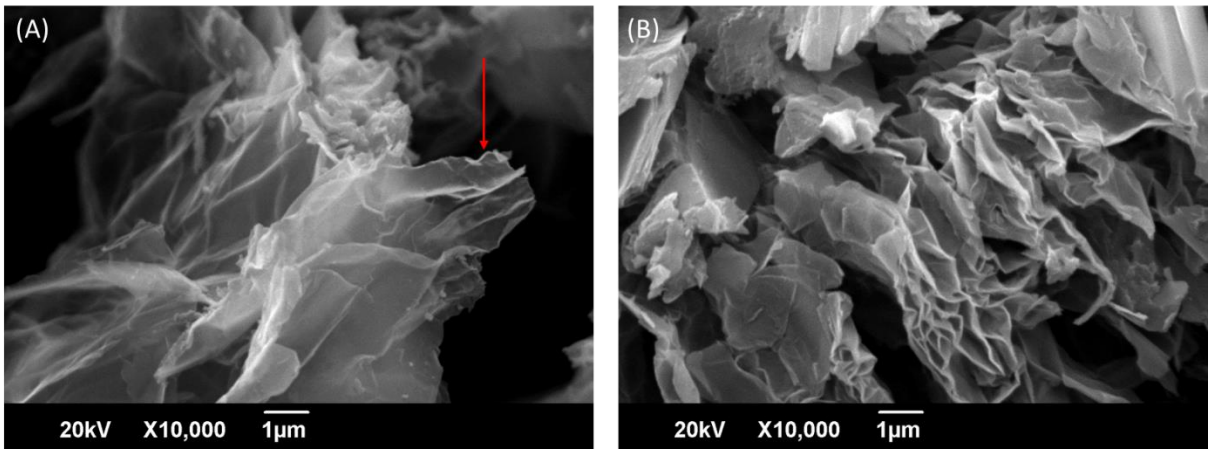

Fig. 9 SEM images of (A) single layer and (B) few-layer graphene sheets after electrochemical exfoliation process.

Figure 10 shows the product of the exfoliation process of graphite mines under optimal conditions presented in Table 5. The presence of graphene sheets of irregular shape and non-uniform thicknesses, according with previous results in literature for this type of synthesis, can be observed in Figure 10 (Parvez et al., 2014).

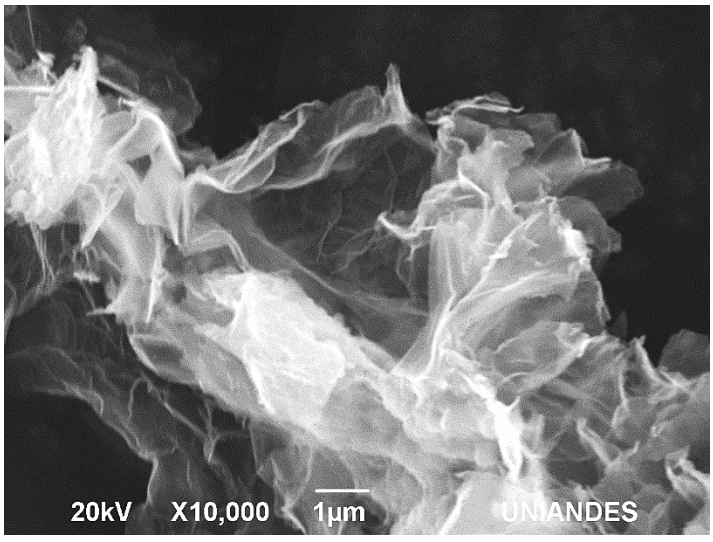

Fig. 10 Micrograph graphene obtained using optimal conditions via electrochemical exfoliation.

3.3.1.2. Fourier transform infrared spectroscopy (FTIR)

FTIR transmission spectrum for graphene in aqueous solution in 400 to 4000 cm^{-1} is presented in Figure 11, it can be identified different peaks that correspond to different functional groups in the sample. There are two types of C-H bonds, 2304.09 and 2385.58 cm^{-1} corresponding to stretching vibration while 1451.65 cm^{-1} correspond to the bending vibration because of water absorption by graphene, 1636.45 and 1093.09 cm^{-1} peaks in the medium frequency area correspond to C=C aromatic groups and C-O of carbonyl groups; 3247.43 cm^{-1} correspond to O-H groups because of water in the solution. Table 9 shows a comparison between own values and those reported in literature (Aldosari, Othman, & Alsharaeh, 2013; Bykkam, Rao, Chakra, & Thunugunta, 2013; Jibrael & Mohammed, 2016a; Zaaba et al., 2017), supporting that the electrochemical exfoliation of graphite to produce graphene was appropriate.

Table 9 Comparison of Wavenumber values of optimal graphene with literature (Aldosari et al., 2013; Bykkam et al., 2013; Jibrael & Mohammed, 2016a; Zaaba et al., 2017).

	Wavenumber (cm^{-1})	
Functional group	Literature	This work
	2865.67	2106.46
C-H	2918.4	2121.36
	1465.95	1451.95
C=C	1643.41	1636.29
C-O	1095.6	1092.79
O-H	3446.91	3272.46

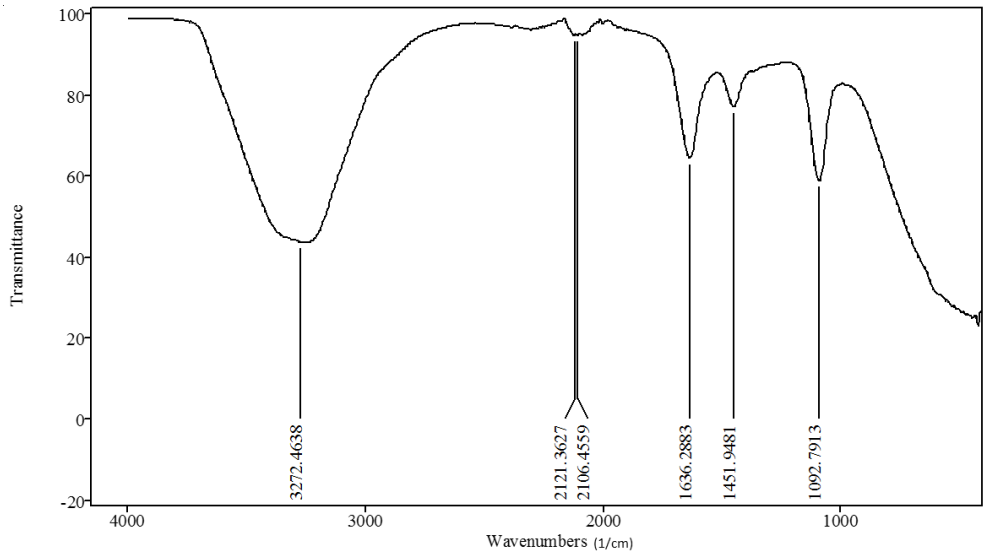

Fig. 11 FTIR spectrum of graphene in aqueous solution.

3.3.1.3. X-Ray diffraction (XRD)

Figure 12 shows XRD patterns of graphite and graphene after electrochemical process. As can be seen in the figure, a weak peak appeared at 2θ = 54.6° for graphite (a) that corresponds to the (1 0 1) plane and is absent in the graphene diffractogram is disappeared in graphene pattern (b) (Hadi, Karimi-Sabet, Moosavian, & Ghorbanian, 2016). Main diffraction peak of both spectrums are located at 2θ = 26.5° which relates to (0 0 2) crystal plane of carbon with different intensities and interlayer distance of 0.94 Å using Bragg equation, this indicates that exfoliation process of graphite mines produce few layer graphene (Hadi et al., 2016).

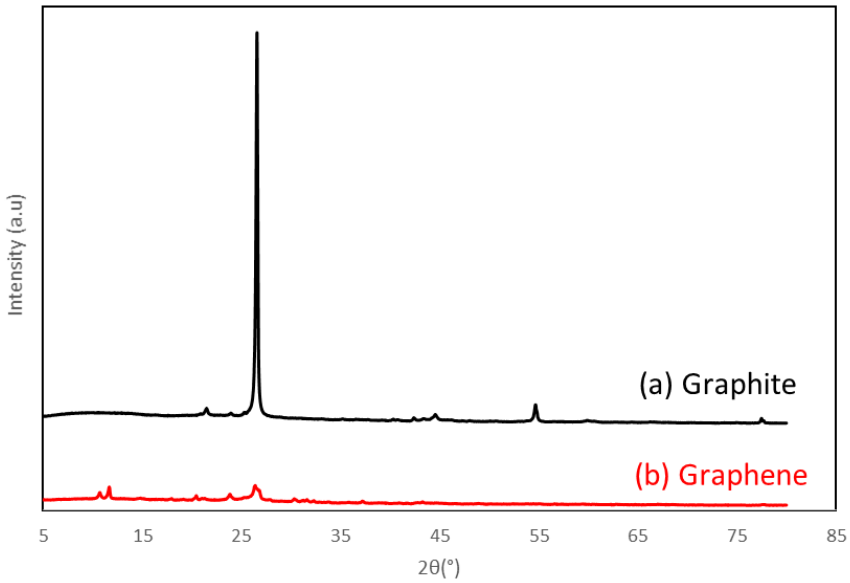

Fig. 12 XRD Patterns of (a) graphite and (b) electrochemical exfoliated graphene

3.3.2. Nylon nanowires characterization

3.3.2.1. Scanning electron microscopy (SEM)

Fig. 13 shows a micrograph image proving the nanowire nylon distribution.. Average diameter of nanowires is 69±15 nm while what the model for these conditions predicts is 65.83±12 nm clearly demonstrating the consistency of the proposed model.

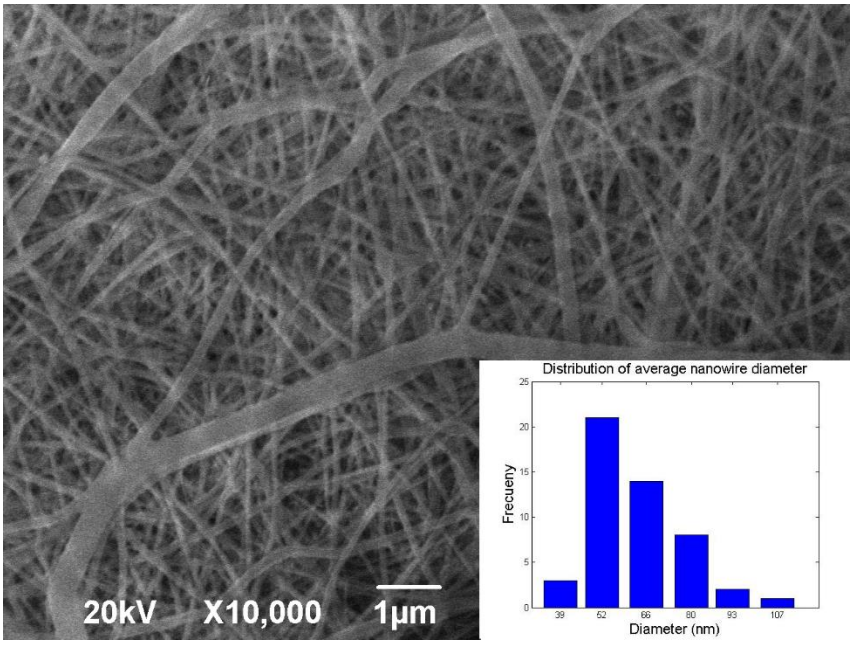

Fig. 13 Micrograph of the optimal nylon nanowire material. Insert: Diameter distribution in micrograph.

3.3.2.2. Fourier transform infrared spectroscopy (FTIR)

Table 10 shows a comparison between wavelength values reported in literature and those obtained for nylon nanowires, proving that during electrospinning process there was no chemical transformation due formic acid used as a solvent. Also Fig. 14 shows FTIR spectrum for nylon nanowires.

Table 10 Comparison between wavenumber values reported in literature (Charles, Ramkumaar, Azhagiri, & Gunasekaran, 2009) and the present work

	Wavenumber (cm^{-1})	
Functional group	Literature	This work
O-H	3250	3294.67
C-H	3050	3060.94
	2950	2935.70
	2850	2866.18
C=C	1620	1635.01
N-H	1590	1538.34
C=C	1450	1461.81
C-O	1230	1263.32
	1200	1199.81

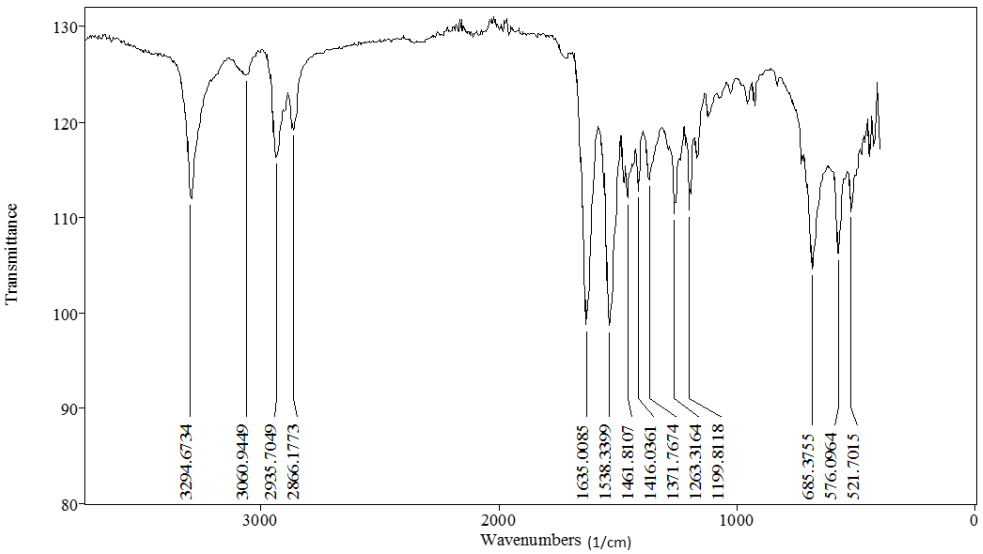

Fig. 14 FTIR spectrum of nylon nanowires

3.3.3. Optimal nylon nanowires/graphene composite

3.3.3.1. Scanning electron microscopy (SEM)

In Figure 15 a nylon nanowires/graphene composite can be observed. It is possible to see that graphene is not crossed but is bonded and surrounding the nylon nanowires. This suggests that graphene has hydrophilic groups that can interact with amide groups of nylon; being according with data reported by Menchaca-Campos and coworkers (Menchaca-Campos et al., 2013).

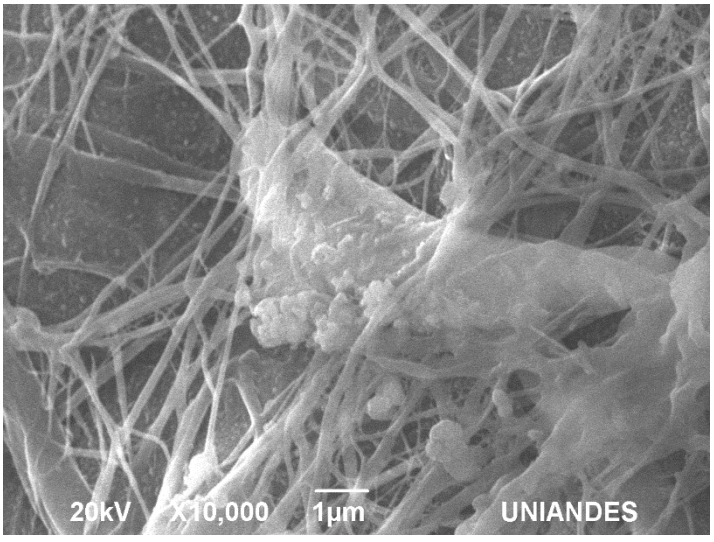

Fig. 15 Micrograph of optimal nylon nanowires/graphene composite material

3.3.3.2. Atomic force microscopy (AFM)

Nylon nanowires/graphene composite were analyzed using atomic force microscope. This material presented two zones in particular, the first one is observed in Figure 16 (A), that shows typical nanowires obtained from electrospinning process with roughness of 68.1 nm in diameter; Fig. 16 (C) also shows the roughness profile in the sample (black line in Figure 16(A)). Figure 16 (B) shows sections where graphene can be found, agglomerations are present in the same sample, because there are clusters of graphene layers between nylon, roughness profile of this section is presented in Figure 16 (D) where principal roughness parameter R_a was 113.5 nm. The difference in roughness between both sections of the sample was 45.4 nm.

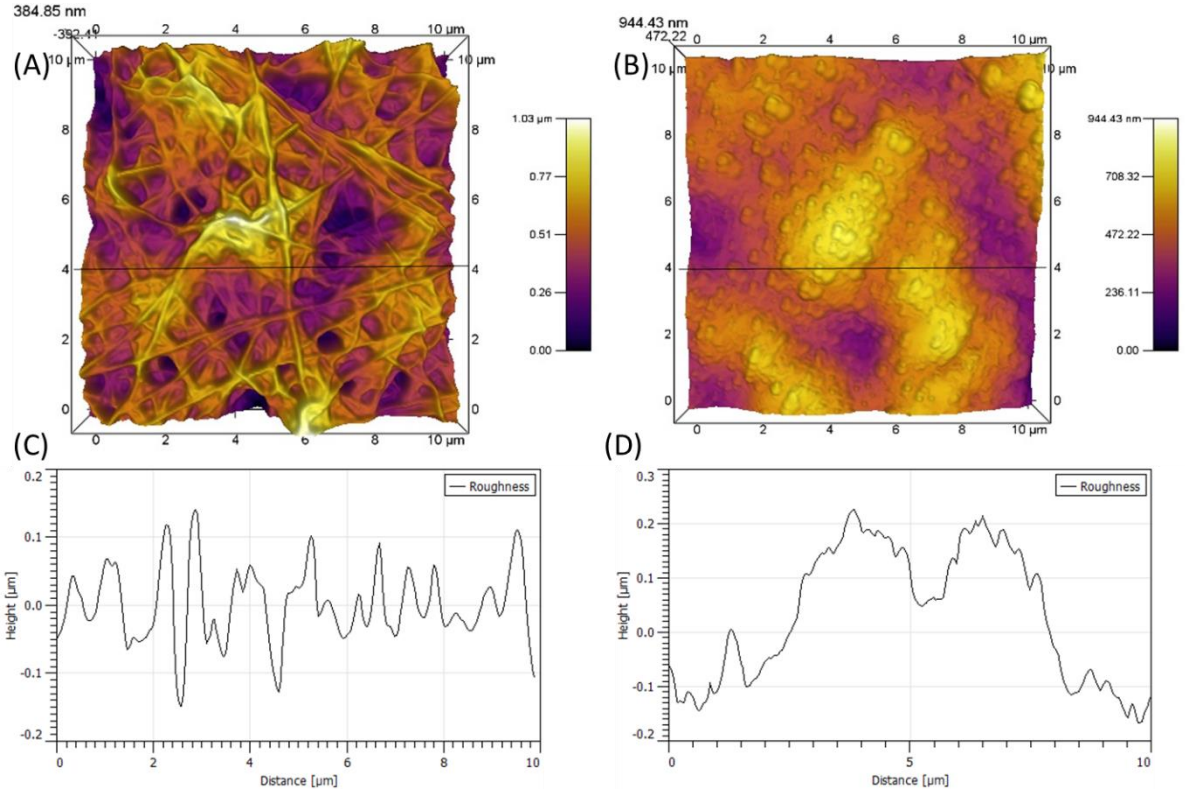

Fig. 16 Topography of nylon nanowires/graphene composite employing AFM. (A) Isolated nanowires and (B) nylon nanowires/graphene composite, and (C) - (D) show line scan data corresponding to the black lines in (A) and (B), respectively.

3.3.3.3. Fourier transform infrared spectroscopy (FTIR)

Figure 17 shows FTIR spectrum for nylon nanowires/graphene composite material, there is no chemical changes when graphene is added to polymeric matrix; however, it can be seen that the spectrum changes the intensity with respect to the pristine nylon nanowires, which indicates the presence of another component in the sample, in this case graphene.

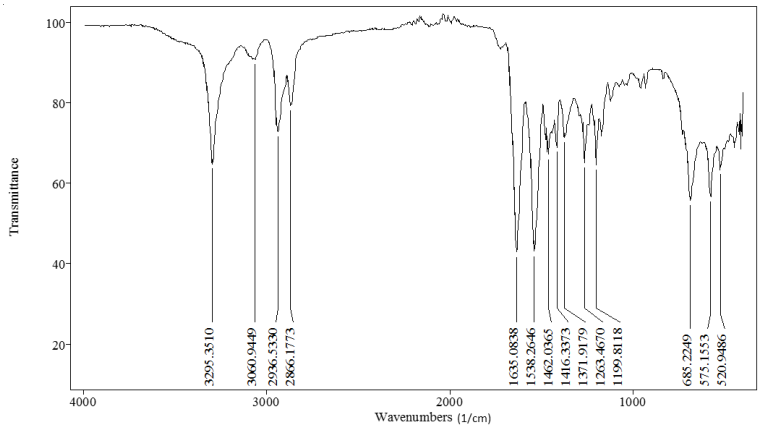

Fig. 17 FTIR spectrum for nylon nanowires/graphene composite

3.3.3.4. X-Ray diffraction (XRD)

Figure 18 shows comparison between XRD patterns of nylon nanowires and nylon nanowires/graphene composite. As can be seen, the addition of 1% of graphene in to the mixture, decreases the intensity of 20.45° and 24.53° 2θ peaks and increase 28.89° 2θ peak, it is because the addition of graphene gives a high proportion of the plane (0 0 2) and decrease the intensity of the characteristic nylon plane in the sample (Ozgit-Akgun et al., 2015).

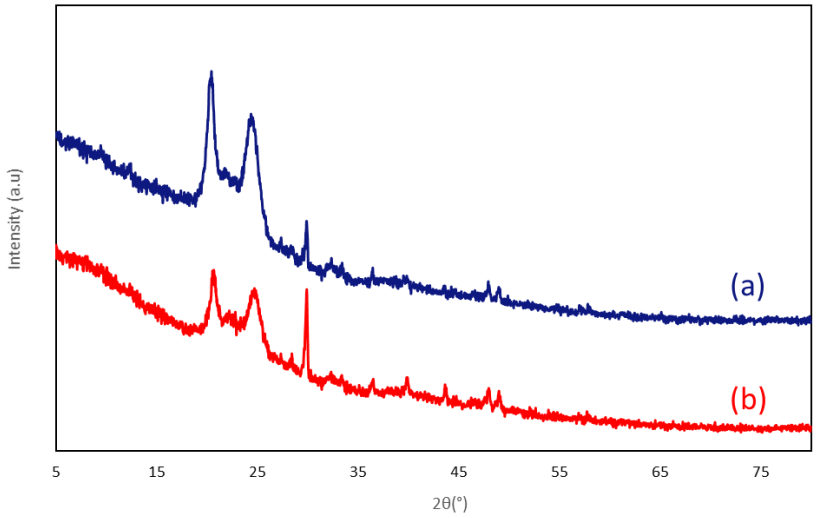

Fig. 18 X-Ray diffraction patterns of (a) nylon nanowires and (b) nylon nanowires/graphene composite.

3.3.3.5. Antimicrobial test

Figure 19 shows antimicrobial activity of nylon nanowires/graphene composite for *Micrococcus luteus*, section (b) in this figure revels inhibition halo with 0.92 cm of diameter, also section (c) revels partial inhibition halo. Composite material film does not have any antibiotic and for this

reason this material inhibits activity for this microorganism, this property is attributed to graphene in the polymeric matrix (Santos et al., 2011). It is important to point out, that results from antimicrobial activity of nylon nanowires/graphene composite are unpublished to the date.

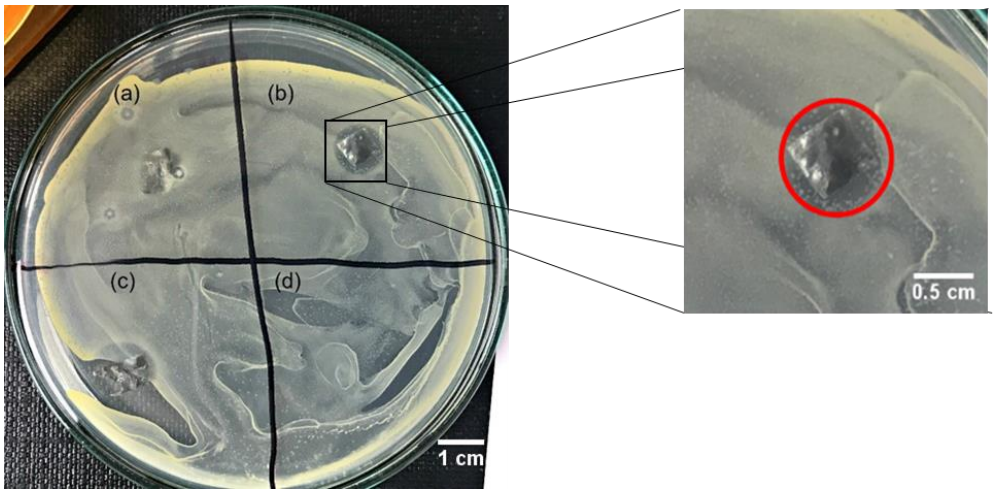

Fig. 19 Culture of *Micrococcus luteus in TSA agar where* (a), (b), (c) are anttimicrobial activity of nylon nanowires/graphene composite, (d) positive blank. Extended area demostrates inhibition halo.

3.3.3.6. UV blocking test

Ultraviolet light is harmful to living organisms. Due to the increasing deterioration of the ozone layer, it cannot block ultraviolet rays from the sun properly (Pant et al., 2011). By this reason, it is needded to explore new materials that have the capacity to absorb ultraviolet rays. To investigate UV blocking properties of nylon nanowires/graphene composites a measure process was carried out at room temperature. Figure 20 shows absorbance spectra of nylon nanowires and nylon nanowires/graphene composites. It is possible to realize about, the addition of 1% of graphene the absorption of light of different wavelengths increases by an average of 70% $\left(\frac{Nanowires\ absorbance}{Composite\ absorbance} * 100\right)$ because of the absorbance of UV light for transferring the electron from the valance band to the conduction band. There are similar reports in literature with other composites (Pant et al., 2011). Above results demonstrate the possibility to use nylon nanowires/graphene composite material in textile industries taking advantage of the UV blocking property.

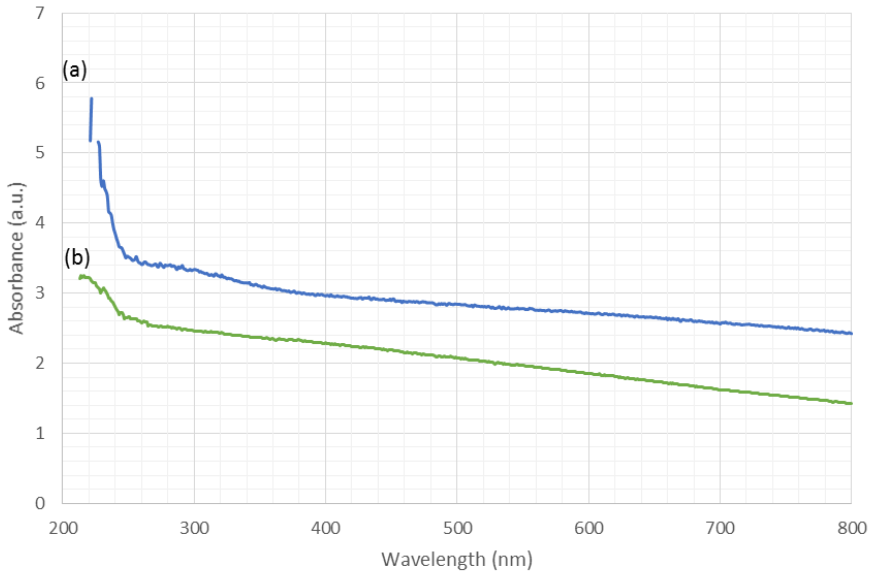

Fig. 20 UV-visible spectrum for (a) nylon nanowires/graphene composite with 1% of graphene and (b) nylon nanowires

4. CONCLUSIONS

In the present study, the optimal conditions to produce graphene and nylon nanowires were determined., for which it was obtained that applied voltage equal to 11.45 V and 0.68 M concentration of $(NH_4)_2SO_4$ gives a 67.21% of yield in graphene production and applied voltage equal to 27 kV, flow equal to 2.3 mL/h and collector-needle distance of 11.40 cm for nylon nanowires production gives average diameter fiber of 65.83 ±12.09. The properties of nanometric materials were confirmed via different characterizations as SEM, AFM, FTIR and XRD. Optimal materials were used to fabricate composite via electrospinning process. Composite material was analyzed by SEM, AFM, FTIR, XRD, UV-visible spectroscopy and antimicrobial. This material has the ability of blocking UV rays 70% times more than pristine nylon nanowires, and also, present antimicrobial activity for *Micrococcus luteus*. Further studies about conductivity assessment can support that this material can be used in e-textile industry. Finally, the techniques presented in this work can be potential ways to recycle nylon in order to avoid polymer contamination.

5. ACKNOWLEDGEMENTS

The authors are grateful to Universidad Jorge Tadeo Lozano for supporting this work, to Universidad Nacional de Colombia and Universidad Central for supporting XRD and AFM characterizations, respectively.

REFERENCES

Aldosari, M., Othman, A., & Alsharaeh, E. (2013). Synthesis and Characterization of the in Situ Bulk Polymerization of PMMA Containing Graphene Sheets Using Microwave Irradiation. *Molecules*, *18*(3), 3152–3167. https://doi.org/10.3390/molecules18033152

Bykkam, S., Rao, V. K., Chakra, S. C., & Thunugunta, T. (2013). SYNTHESIS AND CHARACTERIZATION OF GRAPHENE OXIDE AND ITS ANTIMICROBIAL ACTIVITY AGAINST Klebseilla AND Staphylococus. *International Journal of Advanced Biotechnology and Research*, *4*(1), 2278–599. Retrieved from http://www.bipublication.com

Charles, J., Ramkumaar, G. R., Azhagiri, S., & Gunasekaran, S. (2009). FTIR and thermal studies on nylon-66 and 30% glass fibre reinforced nylon-66. *Journal of Chemistry*, *6*(1), 23–33.

Chen, K., Xue, D., & Komarneni, S. (2017). Nanoclay assisted electrochemical exfoliation of pencil core to high conductive graphene thin-film electrode. *Journal of Colloid and Interface Science*, *487*, 156–161. https://doi.org/http://doi.org/10.1016/j.jcis.2016.10.028

Deitzel, J. (2002). Electrospinning of polymer nanofibers with specific surface chemistry. *Polymer*, *43*(3), 1025–1029. https://doi.org/10.1016/S0032-3861(01)00594-8

El-Newehy, M. H., Al-Deyab, S. S., Kenawy, E.-R., & Abdel-Megeed, A. (2011). Nanospider Technology for the Production of Nylon-6 Nanofibers for Biomedical Applications. *Journal of Nanomaterials*, *2011*, 1–8. https://doi.org/10.1155/2011/626589

Hadi, A., Karimi-Sabet, J., Moosavian, S. M. A., & Ghorbanian, S. (2016). Optimization of graphene production by exfoliation of graphite in supercritical ethanol: A response surface methodology approach. *The Journal of Supercritical Fluids*, *107*, 92–105. https://doi.org/10.1016/j.supflu.2015.08.022

Huang, Z.-M., Zhang, Y.-Z., Kotaki, M., & Ramakrishna, S. (2003). A review on polymer nanofibers by electrospinning and their applications in nanocomposites. *Composites Science and Technology*, *63*(15), 2223–2253. https://doi.org/10.1016/S0266-3538(03)00178-7

Ji, X., Xu, Y., Zhang, W., Cui, L., & Liu, J. (2016). Review of functionalization, structure and properties of graphene/polymer composite fibers. *Composites Part A: Applied Science and Manufacturing*, *87*, 29–45. https://doi.org/http://dx.doi.org.ezproxy.utadeo.edu.co/10.1016/j.compositesa.2016.04.011

Jibrael, R. I., & Mohammed, M. K. A. (2016a). Production of graphene powder by electrochemical exfoliation of graphite electrodes immersed in aqueous solution. *Optik - International Journal for Light and Electron Optics*, *127*(16), 6384–6389. https://doi.org/10.1016/j.ijleo.2016.04.101

Jibrael, R. I., & Mohammed, M. K. A. (2016b). Production of graphene powder by electrochemical exfoliation of graphite electrodes immersed in aqueous solution. *Optik* -

International Journal for Light and Electron Optics, *127*(16), 6384–6389. https://doi.org/http://dx.doi.org.ezproxy.utadeo.edu.co/10.1016/j.ijleo.2016.04.101

Jr, W. S. H., & Offeman, R. E. (1958). Preparation of graphitic oxide. *Journal of the American Chemical Society*, *80*(6), 1339.

Ki, C. S., Baek, D. H., Gang, K. D., Lee, K. H., Um, I. C., & Park, Y. H. (2005). Characterization of gelatin nanofiber prepared from gelatin–formic acid solution. *Polymer*, *46*(14), 5094–5102. https://doi.org/10.1016/j.polymer.2005.04.040

Laurencin, C. T., Ambrosio, A. M. A., Borden, M. D., & Cooper Jr, J. A. (1999). Tissue engineering: orthopedic applications. *Annual Review of Biomedical Engineering*, *1*(1), 19–46.

Lee, C., Wei, X., Kysar, J. W., & Hone, J. (2008). Measurement of the Elastic Properties and Intrinsic Strength of Monolayer Graphene. *Science*, *321*(5887). Retrieved from http://science.sciencemag.org/content/321/5887/385

Li, X., Magnuson, C. W., Venugopal, A., Tromp, R. M., Hannon, J. B., Vogel, E. M., … Ruoff, R. S. (2011). Large-area graphene single crystals grown by low-pressure chemical vapor deposition of methane on copper. *Journal of the American Chemical Society*, *133*(9), 2816–2819.

Li, Z., & Wang, C. (2013). Effects of Working Parameters on Electrospinning (pp. 15–28). Springer Berlin Heidelberg. https://doi.org/10.1007/978-3-642-36427-3_2

Lu, X., Yu, M., Huang, H., & Ruoff, R. S. (1999). Tailoring graphite with the goal of achieving single sheets. *Nanotechnology*, *10*(3), 269.

Menchaca-Campos, C., García-Pérez, C., Castañeda, I., García-Sánchez, M. A., Guardián, R., & Uruchurtu, J. (2013). Nylon/graphene oxide electrospun composite coating. *International Journal of Polymer Science*, *2013*.

Necas, D., & Klapetek, P. (2012). Gwyddion: an open-source software for {SPM} data analysis. *Central European Journal of Physics*, *10*(1), 181–188. https://doi.org/10.2478/s11534-011-0096-2

Nirmala, R., Navamathavan, R., El-Newehy, M. H., & Kim, H. Y. (2011). Preparation and electrical characterization of polyamide-6/chitosan composite nanofibers via electrospinning. *Materials Letters*, *65*(3), 493–496. https://doi.org/10.1016/j.matlet.2010.10.066

Novoselov, K. S., Geim, A. K., Morozov, S. V, Jiang, D., Zhang, Y., Dubonos, S. V, … Firsov, A. A. (2004). Electric Field Effect in Atomically Thin Carbon Films. *Science*, *306*(5696), 666–669. https://doi.org/10.1126/science.1102896

Ozgit-Akgun, C., Kayaci, F., Vempati, S., Haider, A., Celebioglu, A., Goldenberg, E., … Biyikli,

N. (2015). Fabrication of flexible polymer–GaN core–shell nanofibers by the combination of electrospinning and hollow cathode plasma-assisted atomic layer deposition. *J. Mater. Chem. C*, *3*(20), 5199–5206. https://doi.org/10.1039/C5TC00343A

Pant, H. R., Bajgai, M. P., Nam, K. T., Seo, Y. A., Pandeya, D. R., Hong, S. T., & Kim, H. Y. (2011). Electrospun nylon-6 spider-net like nanofiber mat containing TiO2 nanoparticles: A multifunctional nanocomposite textile material. *Journal of Hazardous Materials*, *185*(1), 124–130. https://doi.org/10.1016/j.jhazmat.2010.09.006

Parvez, K., Wu, Z.-S., Li, R., Liu, X. J., Graf, R., Feng, X., & Müllen, K. (2014). Exfoliation of graphite into graphene in aqueous solutions of inorganic salts. *Journal of the American Chemical Society*, *136*(16), 6083–6091.

Pedicini, A., & Farris, R. J. (2004). Thermally induced color change in electrospun fiber mats. *Journal of Polymer Science Part B: Polymer Physics*, *42*(5), 752–757. https://doi.org/10.1002/polb.10711

Ray, S. C. (2015a). Chapter 1 - Application and Uses of Graphene. In S. C. Ray (Ed.) (pp. 1–38). Oxford: William Andrew Publishing. https://doi.org/http://dx.doi.org.ezproxy.utadeo.edu.co/10.1016/B978-0-323-37521-4.00001-7

Ray, S. C. (2015b). Chapter 2 - Application and Uses of Graphene Oxide and Reduced Graphene Oxide. In S. C. Ray (Ed.) (pp. 39–55). Oxford: William Andrew Publishing. https://doi.org/http://dx.doi.org.ezproxy.utadeo.edu.co/10.1016/B978-0-323-37521-4.00002-9

Ren, G., Zhang, Z., Zhu, X., Ge, B., Guo, F., Men, X., & Liu, W. (2013). Influence of functional graphene as filler on the tribological behaviors of Nomex fabric/phenolic composite. *Composites Part A: Applied Science and Manufacturing*, *49*, 157–164.

Reneker, D., & Chun, I. (1996). Nanometre diameter fibres of polymer, produced by electrospinning. - *Nanotechnology*.

Santos, C. M., Tria, M. C. R., Vergara, R. A. M. V., Ahmed, F., Advincula, R. C., Rodrigues, D. F., … Firsov, A. A. (2011). Antimicrobial graphene polymer (PVK-GO) nanocomposite films. *Chemical Communications*, *47*(31), 8892. https://doi.org/10.1039/c1cc11877c

Schneider, C. A., Rasband, W. S., & Eliceiri, K. W. (2012). NIH Image to ImageJ: 25 years of image analysis. *Nature Methods*, *9*(7), 671–675.

Scopus. (n.d.). Journal title list.

Stankovich, S., Dikin, D. A., Dommett, G. H. B., Kohlhaas, K. M., Zimney, E. J., Stach, E. A., … Ruoff, R. S. (2006). Graphene-based composite materials. *Nature*, *442*(7100), 282–286.

Stoller, M., Park, S., Zhu, Y., An, J., & Ruoff, R. (2008). Graphene-Based Ultracapacitors. -

Nano Letters. https://doi.org/- 10.1021/nl802558y

Wang, J., Manga, K. K., Bao, Q., & Loh, K. P. (2011). High-Yield Synthesis of Few-Layer Graphene Flakes through Electrochemical Expansion of Graphite in Propylene Carbonate Electrolyte. *Journal of the American Chemical Society*, *133*(23), 8888–8891. https://doi.org/10.1021/ja203725d

Yu, P., Lowe, S. E., Simon, G. P., & Zhong, Y. L. (2015). Electrochemical exfoliation of graphite and production of functional graphene. *Current Opinion in Colloid & Interface Science*, *20*(5), 329–338. https://doi.org/http://doi.org/10.1016/j.cocis.2015.10.007

Yuan, X., Zhang, Y., Dong, C., & Sheng, J. (2004). Morphology of ultrafine polysulfone fibers prepared by electrospinning. *Polymer International*, *53*(11), 1704–1710. https://doi.org/10.1002/pi.1538

Zaaba, N. I., Foo, K. L., Hashim, U., Tan, S. J., Liu, W.-W., & Voon, C. H. (2017). Synthesis of Graphene Oxide using Modified Hummers Method: Solvent Influence. *Procedia Engineering*, *184*, 469–477. https://doi.org/10.1016/j.proeng.2017.04.118

Zhang, C., Yuan, X., Wu, L., Han, Y., & Sheng, J. (2005). Study on morphology of electrospun poly(vinyl alcohol) mats. *European Polymer Journal*, *41*(3), 423–432. https://doi.org/10.1016/j.eurpolymj.2004.10.027

Zhang, S., Shim, W. S., & Kim, J. (2009). Design of ultra-fine nonwovens via electrospinning of Nylon 6: Spinning parameters and filtration efficiency. *Materials & Design*, *30*(9), 3659–3666. https://doi.org/10.1016/j.matdes.2009.02.017

Zhong, Y. L., & Swager, T. M. (2012). Enhanced electrochemical expansion of graphite for in situ electrochemical functionalization. *Journal of the American Chemical Society*, *134*(43), 17896–17899.

Zhong, Y. L., Tian, Z., Simon, G. P., & Li, D. (2015). Scalable production of graphene via wet chemistry: progress and challenges. *Materials Today*, *18*(2), 73–78. https://doi.org/10.1016/j.mattod.2014.08.019